

Low-Temperature Superplasticity in Aluminum Alloys Processed by Equal-Channel Angular Pressing

Satoshi Ota¹, Hiroki Akamatsu¹, Koji Neishi¹, Minoru Furukawa²,
Zenji Horita¹ and Terence G. Langdon³

¹Department of Materials Science and Engineering, Faculty of Engineering, Kyushu University, Fukuoka 812-8581, Japan

²Department of Technology, Fukuoka University of Education, Munakata, Fukuoka 811-4192, Japan

³Departments of Aerospace & Mechanical Engineering and Materials Science,
University of Southern California, Los Angeles, CA 90089-1453, USA

Equal-channel angular pressing (ECAP) was applied to achieve grain refinement of Al–3 mass%Mg alloys containing 0.2 mass%Sc, 0.2 mass%Fe or 0.1 mass%Zr. The thermal stability of the fine-grained structures was examined by conducting static annealing experiments. The fine grain sizes produced by ECAP were essentially retained up to a temperature of 523 K for the Fe-containing and Zr-containing alloys and up to a temperature as high as 773 K for the Sc-containing alloy. The three alloys with Sc, Fe and Zr additions were pulled to failure in tension at 523 K corresponding to $0.59T_m$, where T_m is the absolute melting point of the alloy, and maximum elongations of $\sim 640\%$, $\sim 370\%$ and $\sim 390\%$ were obtained at an initial strain rate of $3.3 \times 10^{-4} \text{ s}^{-1}$, respectively. Such elongations resulted in more than three times or approximately twice the elongation achieved in a binary Al–3%Mg alloy. It is shown that either Fe or Zr may be used as an alternative element in place of Sc to attain low temperature superplasticity. Tensile testing was also conducted on the Sc-containing ternary alloy at a temperature as low as 473 K corresponding to $0.54T_m$. A maximum elongation of $\sim 420\%$ was attained at an initial strain rate of $3.3 \times 10^{-4} \text{ s}^{-1}$. This appears to be the lowest homologous temperature reported to date for superplasticity of Al-based alloys.

(Received May 20, 2002; Accepted August 7, 2002)

Keywords: superplasticity, equal-channel angular pressing (ECAP), aluminum–magnesium alloys, submicrometer grains, tensile test

1. Introduction

In order to attain superplasticity, it is important to produce small grains which have sizes generally below the range of $\sim 10 \mu\text{m}$.¹⁾ Furthermore, these small grains should be stable at higher temperatures as the superplastic flow occurs through a thermally-activated process.¹⁾ If the grain size is reduced to the submicrometer range, the superplasticity may appear at lower temperatures and/or higher strain rates²⁾ and this is important for the application of superplasticity in industrial forming operations.

It was shown that such small grains can be produced using a process known as equal-channel angular pressing (ECAP)^{3–5)} where a sample is pressed through a channel having an equal cross-section but bent into an L-shaped configuration in a die.⁶⁾ A large shear strain is introduced in the sample when the material passes through the corner of the L-shaped channel. Since the cross-section remains unchanged with this process even after the shear strain is introduced, repetitive pressing is feasible and a large strain is accumulated in the sample. The microstructure evolves into a fine-grained structure having high-angle boundaries as the pressing is repeated.^{7,8)} The advantage of the ECAP process is that grain refinement is achieved in a bulk form of samples, permitting scale-up for commercial use.⁹⁾

There are successful applications of the ECAP process for production of superplastic alloys at low temperatures and/or with high strain rates. For low-temperature superplasticity, Valiev *et al.*¹⁰⁾ first reported that an ECAP-processed Al–4 mass%Cu–0.5 mass%Zr alloy exhibits an elongation of $> 250\%$ at a temperature of 493 K which corresponds to $0.57T_m$ where T_m is the melting point of the alloy.¹¹⁾ Low-

temperature superplasticity was also reported in an AZ91 Mg-based alloy by Mabuchi *et al.*¹²⁾ and a Cu–38%Zn–3%Sn alloy by Neishi *et al.*¹³⁾ with maximum elongations of $\sim 300\%$ at $0.58T_m$ for the former alloy and of 675% at $0.51T_m$ for the latter alloy.¹¹⁾ For high strain rate superplasticity, several reports are available on ECAP-processed alloys.^{14–18)} Among these reports, Komura *et al.*¹⁸⁾ documented elongations over 1000% on an Al–3%Mg–0.2%Sc alloy with strain rates higher than 10^{-2} s^{-1} at a testing temperature of 673 K. It was also shown¹⁸⁾ that the same alloy yielded superplastic ductility greater than 1000% even at 573 K which corresponds to $0.65T_m$. It may be interesting to examine a lower limit of the temperature where the superplastic ductility appears in this alloy. Thus, the first aim of this study was to perform tensile testing of the Al–3%Mg–0.2%Sc alloy below the temperature of 573 K.

In the study of Komura *et al.* using the Al–3%Mg–0.2%Sc alloy,¹⁸⁾ the addition of Sc was made because it forms finely dispersed particles of Al_3Sc and they effectively inhibit grain growth. However, Sc is a very expensive element and it is desirable to replace it with other common elements such as Fe and Zr in Al alloys. Therefore, the second aim of this study was to examine the presence of any alternative elements for Sc that give rise to superplastic ductility.

2. Experimental Materials and Procedures

2.1 Materials

This study used alloys of Al–3%Mg containing 0.2%Sc, 0.2%Fe or 0.1%Zr including, for comparison, an Al–3%Mg alloy without any addition of a third element. Here, the compositions are given in mass%.

The three ternary alloys were prepared from high purity Al (99.99%), high purity Mg (99.9%) and an Al-X mother alloy with $X = 3\% \text{Sc}$, $51.2\% \text{Fe}$ or $5.1\% \text{Zr}$. The Al-3%Sc alloy was made using an arc-melting furnace in an Ar atmosphere and the Al-51.2%Fe and Al-5.1%Zr alloys were used from ingots available commercially. Ingots of the Al-3%Mg-0.2%Sc, Al-3%Mg-0.2%Fe and Al-3%Mg-0.1%Zr alloys were produced by a melting and casting process to dimensions of $20 \times 60 \times 120 \text{ mm}^3$. Each ingot was homogenized at 753 K for 86.4 ks (24 h) and cut into three billets with dimensions of $18 \times 18 \times 120 \text{ mm}^3$. They were swaged into rods with diameters of 10 mm and cut to lengths of 60 mm. After cutting, the rods were solution-treated for 3.6 ks (1 h) at 883 K for the Al-3%Mg-0.2%Sc alloy, at 873 K for the Al-3%Mg-0.2%Fe alloy and at 880 K for the Al-3%Mg-0.1%Zr alloy. The temperatures for the solution treatment were determined such that they were slightly below the melting temperatures of the alloys measured by a differential scanning calorimeter (DSC). The average grain sizes measured after the solution treatment were ~ 200 , ~ 230 and $\sim 360 \mu\text{m}$, respectively. After the solution treatments, aging was further undertaken on the Al-3%Mg-0.1%Zr alloy at 573 K for 10.8 ks (3 h).

For comparison, rods with dimensions of 10 mm in diameter and 60 mm in length were also made from a cold-rolled Al-3%Mg billet using swaging. The rods were annealed for 3.6 ks (1 h) at 773 K. The average grain size after annealing was $\sim 500 \mu\text{m}$.

To examine the thermal stability of fine-grained structures produced by ECAP, static annealing was undertaken for 3.6 ks (1 h) at temperatures in the range of 373 to 773 K.

2.2 ECAP procedure

The ECAP was conducted at room temperature using a die having angles of 90 degrees at the channel intersection and of 20 degrees for the outer arc of curvature. With such angles, an equivalent strain of ~ 1 is created on each passage of the sample through the die.¹⁹ The pressing was repeated 8 times through route B_C where the sample was rotated in the same sense by 90 degrees between each pass about its longitudinal axis.²⁰ A lubricant containing 5%MoS₂ was used to reduce the friction between the sample and the channel wall.

2.3 Microstructural observations and tensile tests

Small pieces with thicknesses of $\sim 0.4 \text{ mm}$ were sliced from the samples subjected to ECAP including those subsequently subjected to static annealing. The slices were obtained parallel to the Y plane, where the Y plane is defined as the plane parallel to the side face of the as-pressed sample at the exit from the die.⁷ Disks with diameters of 3 mm were cut from the slices and ground to thicknesses of $\sim 0.15 \text{ mm}$. These disks were thinned for transmission electron microscopy (TEM) using a twin-jet electropolishing apparatus in a solution of 20% HClO₄, 10% C₃H₈O₃ and 70% C₂H₅OH. An Hitachi H-8100 transmission electron microscope was operated at an accelerating voltage of 200 kV for microstructural observations.

Tensile specimens were machined with the tensile axes parallel to the longitudinal directions of the ECAP samples. They had lengths of 5 mm, thicknesses of 2 mm and widths of 3 mm for the gauge sections. Tensile tests were conducted in air at

selected temperatures in the range of 473 to 573 K with initial strain rates in the range of 1.0×10^{-4} to $1.0 \times 10^{-1} \text{ s}^{-1}$. There was a period of $\sim 1.8 \text{ ks}$ (30 min) to reach the designated temperature and the specimens were further held for 0.6 ks (10 min) before starting the deformation. The testing temperatures were controlled to within ± 1 degree.

To observe grain structures after the tensile tests, an Hitachi FB-2000 focused ion beam (FIB) apparatus was used. Small pieces with lengths of $\sim 1 \text{ mm}$ were cut from the fractured specimens including the fracture tips. The grain structures were examined at points $\sim 0.3 \text{ mm}$ from the fracture tips.

3. Results

3.1 Microstructures and microstructural stability

Figure 1 shows an as-ECAP microstructure of the Al-3%Mg-0.2%Fe alloy and a selected area electron diffraction (SAED) pattern taken from a region of $6.2 \mu\text{m}$ in diameter. The SAED pattern consists of many diffracted beams forming rings and thus indicates that the grains may be separated by high-angle boundaries. Some grains are equiaxed but some are elongated and there are many grain boundaries which are not well defined. These are typical features observed after severe plastic deformation. It was estimated from observations throughout the sample that an area fraction of $\sim 80\%$ contained a homogeneous equiaxed grain structure but the remaining area consisted of grains which were elongated. Similar microstructures were also observed in the as-ECAP Al-3%Mg-0.1%Zr alloy and they are consistent with the microstructures observed earlier on the as-ECAP Al-3%Mg-0.2%Sc alloy.¹⁸ The average grain sizes estimated from grains where the grain boundaries were rather clear were ~ 0.27 and $\sim 0.19 \mu\text{m}$ for the Al-3%Mg-0.2%Fe and Al-3%Mg-0.1%Zr alloys, respectively, and, as reported earlier,¹⁸ it was $\sim 0.2 \mu\text{m}$ for the Al-3%Mg-0.2%Sc alloy.

A microstructure after statically annealing for 3.6 ks (1 h) at 523 K is shown in Fig. 2 from the Al-3%Mg-0.2%Fe alloy. An SAED pattern taken from a region of $6.2 \mu\text{m}$ in diameter is also included. For this condition, most of the grain boundaries are well defined and may be of high angles according

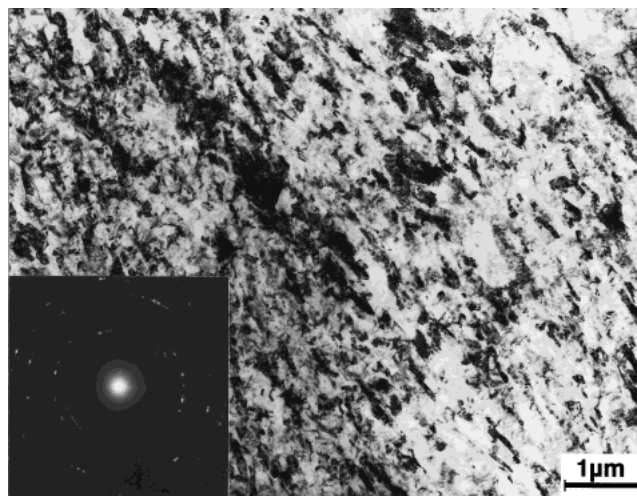


Fig. 1 Microstructure and SAED pattern in the Al-3%Mg-0.2%Fe alloy after 8 passes of ECAP.

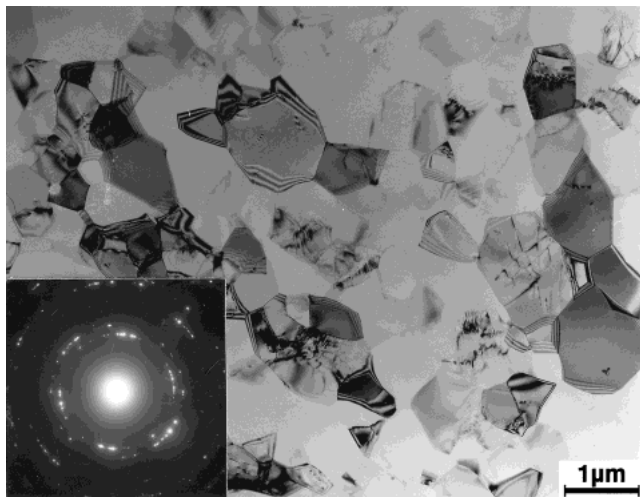


Fig. 2 Microstructure and SAED pattern in the Al-3%Mg-0.2%Fe alloy after 8 passes of ECAP followed by static annealing at 523 K for 3.6 ks (1h).

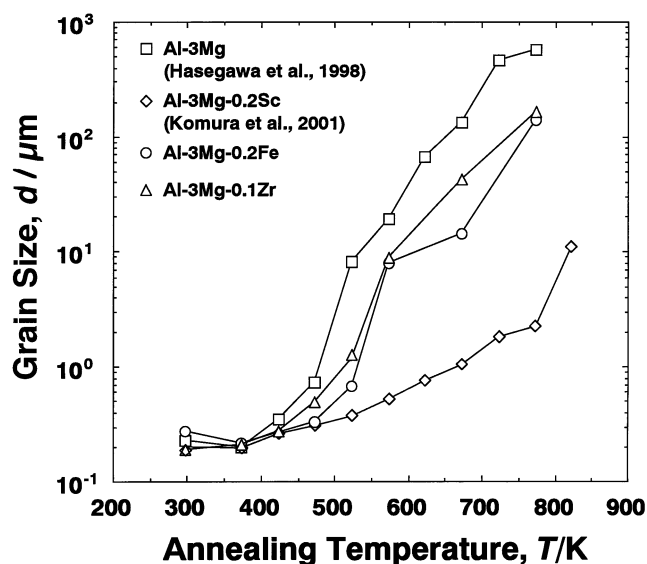


Fig. 3 Variation of grain size with static annealing temperature for Al-3%Mg alloys containing 0.2%Sc, 0.2%Fe and 0.1%Zr including no additional elements. The data for the Al-3%Mg and Al-3%Mg-0.2%Sc alloys are reproduced from published papers.^{18,21)}

to the SAED pattern. When compared with the as-ECAP microstructure shown in Fig. 1, it is apparent that grain growth has occurred due to the annealing. The average grain size was estimated as $\sim 0.68 \mu\text{m}$. Annealing at 573 K led to significant grain growth with an average grain size of $\sim 8.1 \mu\text{m}$. A similar microstructural evolution was observed in the Al-3%Mg-0.1%Zr alloy except that the average grain sizes were $\sim 1.2 \mu\text{m}$ after annealing at 523 K and $\sim 8.8 \mu\text{m}$ after annealing at 573 K. As documented earlier,¹⁸⁾ the microstructural evolution of the Al-3%Mg-0.2%Sc alloy is significantly different from that observed in the Al-3%Mg-0.2%Fe and Al-3%Mg-0.1%Zr alloys. The fine-grained structure was very stable in the Al-3%Mg-0.2%Sc alloy and an average grain size of $\sim 2 \mu\text{m}$ was present after annealing at $\sim 750 \text{ K}$.

The grain growth behavior with respect to the static annealing temperature is more clearly demonstrated in Fig. 3. Here, for comparison, the results of an Al-3%Mg alloy are in-

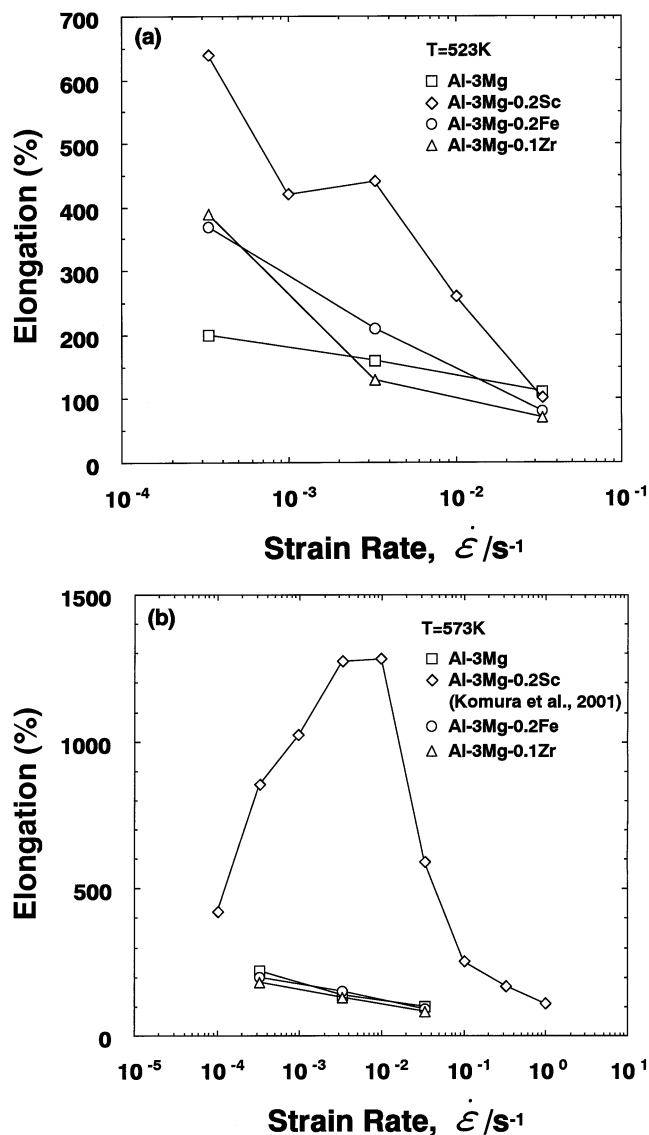


Fig. 4 Elongation to failure versus initial strain rate for Al-3%Mg alloys containing 0.2%Sc, 0.2%Fe and 0.1%Zr including no additional elements after ECAP and pulling to failure at (a) 523 K and (b) 573 K. The data for the Al-3%Mg-0.2%Sc alloy at 573 K are reproduced from a published paper.¹⁸⁾

cluded from an earlier report.²¹⁾ The results of the Al-3%Mg-0.2%Sc alloy are also reproduced from an earlier paper.¹⁸⁾ It is confirmed that the fine-grained structure is retained up to a temperature as high as $\sim 750 \text{ K}$ in the Al-3%Mg-0.2%Sc alloy. The inclusions of Fe or Zr delay the onset of significant grain growth by ~ 50 degrees with respect to the Al-3%Mg binary alloy. It is apparent from Fig. 3 that the effect of Fe and Zr on the inhibition of grain growth is small by comparison with the effect of Sc.

3.2 Tensile testing

Tensile specimens were pulled to failure at 523 K and 573 K, and the elongations to failure are plotted in Figs. 4(a) and (b) as a function of the initial strain rate, respectively. These plots include the results obtained on the Al-3%Mg binary alloy for comparison. Data for the Al-3%Mg-0.2%Sc alloy shown in Fig. 4(b) are reproduced from an earlier study.¹⁸⁾

For the tensile testing at 523 K corresponding to $0.59T_m$, the ductility increases as the strain rate decreases for all alloys. This increase is the largest in the Sc-containing ternary alloy, reaching a maximum elongation of $\sim 640\%$ at a strain rate of $3.3 \times 10^{-4} \text{ s}^{-1}$. The ductility enhancement in the Sc-containing alloy is by a factor of more than three times when compared with the ductility of the binary alloy at lower strain rates. The improvement of the ductility is also significant in the Fe-containing and Zr-containing ternary alloys at a strain rate of $3.3 \times 10^{-4} \text{ s}^{-1}$ where the maximum elongations are $\sim 370\%$ for the Fe-containing alloy and $\sim 390\%$ for the Zr-containing alloy, respectively. These ternary alloys are elongated almost twice as much as the binary alloy although the elongations are nearly the same at and above $3.3 \times 10^{-3} \text{ s}^{-1}$. It is considered that this improvement in the ductility is due to an increasing contribution from superplastic flow.

For the tensile testing at 573 K corresponding to $0.65T_m$, there is no difference in the elongations to failure between the binary and ternary alloys except for the Sc-containing alloy. The small grain sizes are no longer retained at this temperature in the Fe- and Zr-containing alloys as shown in Fig. 3 and therefore the role of grain boundary sliding is insignificant for the overall deformation. By contrast, the total elongation is remarkably high for the Sc-containing alloy, reaching a maximum of $\sim 1280\%$ at a strain rate of $1.0 \times 10^{-2} \text{ s}^{-1}$. Such a large ductility was achieved because the fine-grained structure was stable at this temperature as shown in Fig. 3 and the testing temperature was now increased so that more thermal energy was available to enhance the contribution of grain boundary sliding.

Because the Sc-containing alloy exhibited an elongation of more than 600% at 523 K ($0.59T_m$), tensile testing was further conducted on this alloy at 473 K ($0.54T_m$). The results are plotted in Fig. 5 including those of the binary alloy for comparison. Although the elongation does not increase monotonically with decreasing strain rate, nevertheless the maximum elongation reaches a high value of $\sim 420\%$ at a strain rate of $3.3 \times 10^{-4} \text{ s}^{-1}$. The ductility is thus improved more than twice

with respect to the binary alloy.

The appearances of the specimens after pulling to failure are shown in Fig. 6: (a) and (b) for the Fe- and Zr-containing alloys tested at 523 K, respectively, and (c) for the Sc-containing alloy tested at 473 K. In each photograph, the upper sample is untested and the tested specimens are placed in order from the fastest strain rate at the top to the slowest strain rate at the bottom. For each specimen exhibiting an elongation to failure close to $\sim 400\%$, it is apparent that the flow within the gauge length is reasonably uniform.

Variations of true stress with elongation recorded during testing at 523 K are delineated in Fig. 7 for the Fe- and Zr-containing alloys. For each alloy, the flow stress reaches a maximum but this is followed by a smooth extension of the flow behavior when the specimens were tested at a strain rate of $3.3 \times 10^{-4} \text{ s}^{-1}$.

Figure 8 shows the microstructure of an Fe-containing specimen after testing at a temperature of 523 K with a strain rate of $3.3 \times 10^{-4} \text{ s}^{-1}$. The image was taken at a point $\sim 0.3 \text{ mm}$ from the fracture tip, the tensile axis is horizontal and the side of the tensile specimen lies close to the bottom edge of the photomicrograph. The structure consists of equiaxed grains with grain boundaries clearly defined. The average grain size was measured as $\sim 1.5 \mu\text{m}$ and, when compared with the grain size of $\sim 0.68 \mu\text{m}$ after static annealing for 3.6 ks (1 h) at 523 K shown in Fig. 2, it is apparent that grain growth occurred during testing which lasted for 11.2 ks ($\sim 3 \text{ h}$) to failure. Although cavities are visible as marked by arrows, no grains are elongated along the tensile axis. This suggests that grain boundary sliding occurred and contributed to the overall deformation. Similar grain structures were also observed in the Zr- and Sc-containing alloys after testing to failure at a strain rate of $3.3 \times 10^{-4} \text{ s}^{-1}$ at 523 K and 473 K, respectively.

4. Discussion

Although the strain rate is rather low as $3.3 \times 10^{-4} \text{ s}^{-1}$, the Al-3%Mg-0.2%Sc alloy exhibited superplastic elongations of $\sim 640\%$ at 523 K ($0.59T_m$) and of $\sim 420\%$ at 473 K ($0.54T_m$). This latter temperature of 473 K appears to be the lowest reported to date for superplasticity in any Al-based alloys.

The Al-3%Mg-0.2%Fe and Al-3%Mg-0.1%Zr alloys also yielded superplastic elongations of $\sim 370\%$ and $\sim 390\%$ at 523 K ($0.59T_m$). This demonstrates that Sc can be replaced with Fe or Zr as an alternative third element for the inhibition of grain growth. However, the elongations in these alloys are not as large as in the Sc-containing alloy. This is probably due to the difference in size and distribution of the particles since it has been established that the distribution of Al_3Zr is generally not homogeneous throughout this alloy.²²⁾ In this study, additions of 0.2%Ti, 0.2%Cr and 0.2%Mn to Al-3%Mg were further attempted and tensile tests were performed at a temperature of 523 K for these ternary alloys. Despite similar heat treatments undertaken before ECAP, an elongation above 300% was not achieved in these alloys. The reason for failing to observe superplastic elongations in these alloys may be that diffusion of Ti, Cr and Mn in Al is much lower than the diffusion of Fe and Sc.²³⁾ Because of this low diffusivity,

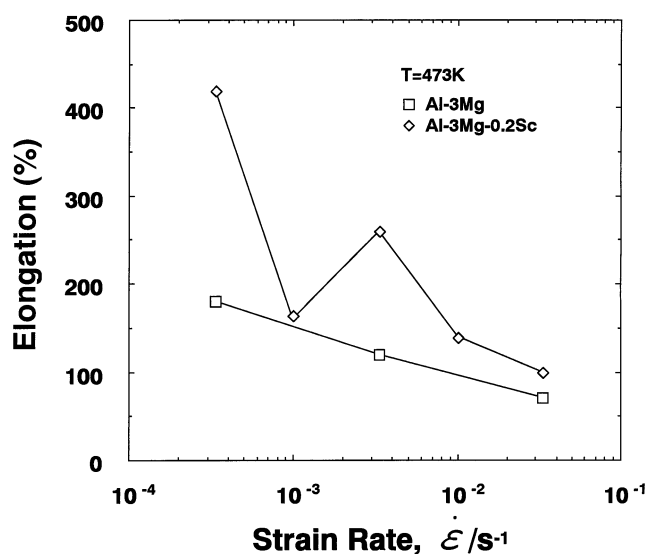


Fig. 5 Elongation to failure versus initial strain rate for the Al-3%Mg-0.2%Sc alloy and the Al-3%Mg alloy after ECAP and pulling to failure at 473 K.

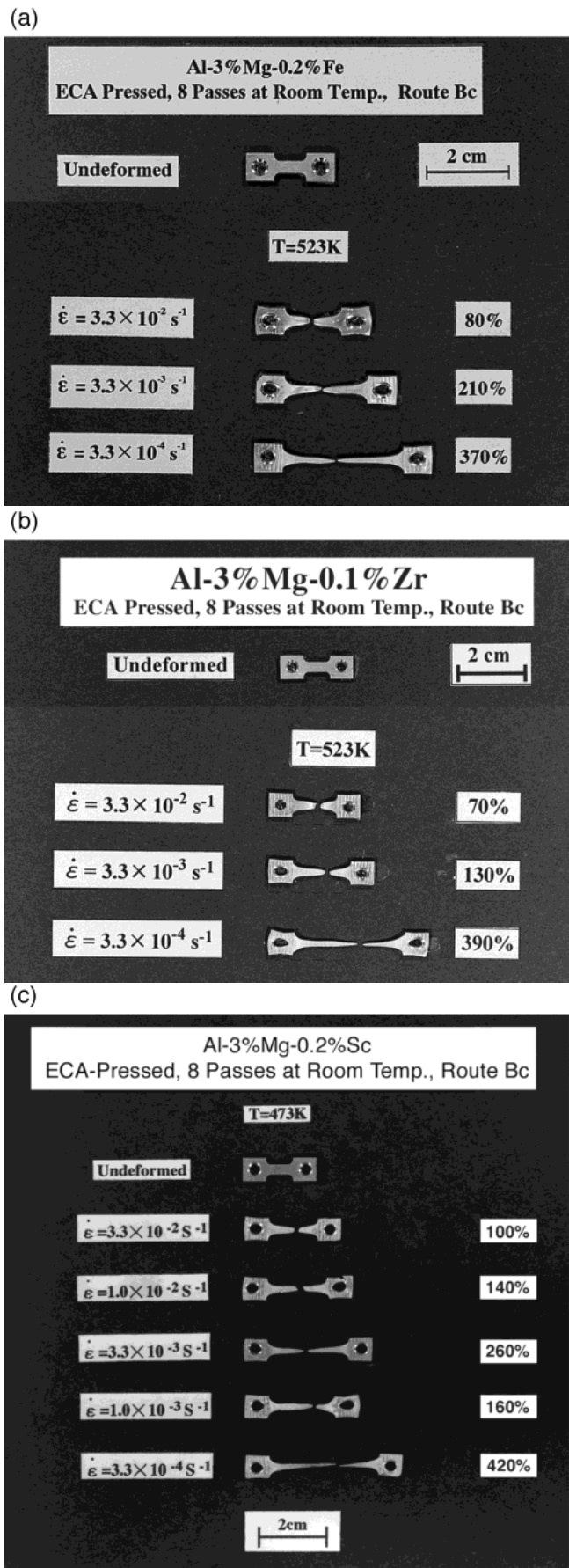


Fig. 6 Appearances of specimens after ECAP and tensile testing (a) at 523 K for the Al-3%Mg-0.2%Fe alloy, (b) at 523 K for the Al-3%Mg-0.1%Zr alloy and (c) at 473 K for the Al-3%Mg-0.2%Sc alloy.

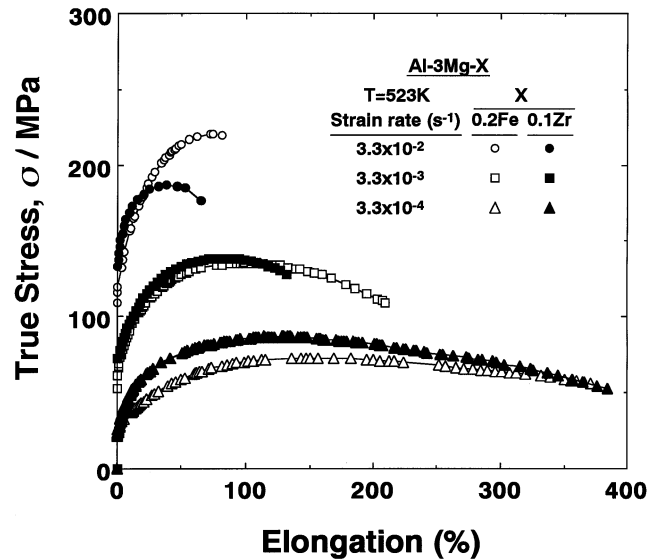


Fig. 7 True stress versus elongation to failure for specimens of the Al-3%Mg-0.2%Fe and Al-3%Mg-0.1%Zr alloys tested at 523 K.

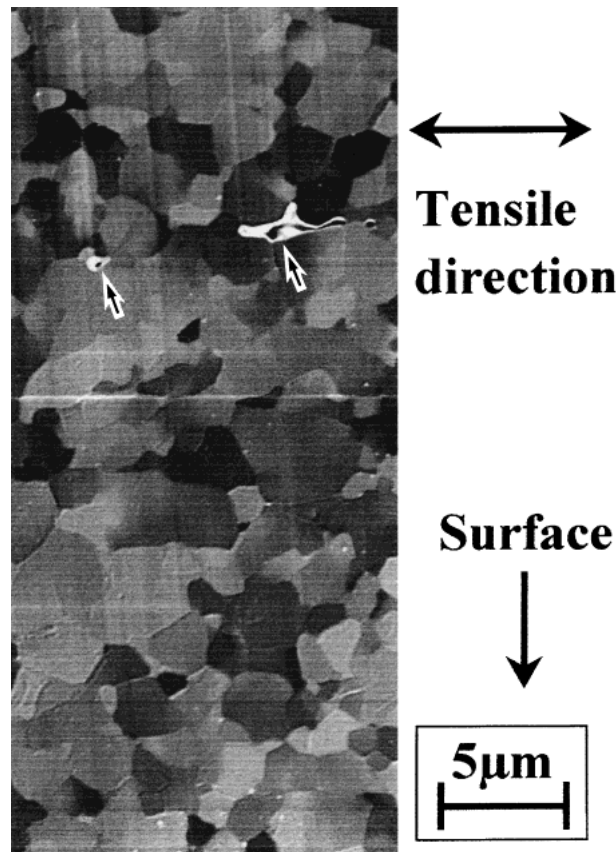


Fig. 8 Microstructure at a point ~0.3 mm from the fracture tip after pulling to failure at 523 K with an initial strain rate of $3.3 \times 10^{-4} \text{ s}^{-1}$ for the Al-3%Mg-0.2%Fe alloy.

there is less opportunity to form particles during ECAP processing. Although the diffusion of Zr in Al is also low, the present study included an aging treatment for 10.8 ks (3 h) at 573 K before ECAP. Without this aging treatment, the Zr-containing alloy yielded an elongation of ~200% at 523 K. Lee *et al.* also reported, with a commercial alloy containing 0.2%Zr, that the maximum elongation at 573 K is only slightly above ~200%.²⁴⁾ Thus, either the presence of par-

ticles before ECAP or the precipitation of particles during ECAP represent an important requirement for achieving superplastic ductilities in these Al-based alloys.

5. Summary and Conclusions

(1) Grain refinement was achieved using an ECAP process to sizes of ~ 0.27 and ~ 0.19 μm for Al–3%Mg–0.2%Fe and Al–3%Mg–0.1%Zr alloys, respectively. These grain sizes were comparable to the value of ~ 0.2 μm achieved earlier for an Al–3%Mg–0.2%Sc alloy.

(2) Static annealing experiments revealed that the fine-grained structures of the ECAP-processed Al–3%Mg–0.2%Fe and Al–3%Mg–0.1%Zr alloys were essentially retained up to a temperature of 523 K but significant grain growth occurred at 573 K for both alloys. This grain growth behavior was very different from that reported in an Al–3%Mg–0.2%Sc alloy where the small grains produced by ECAP were stable up to a temperature of ~ 750 K.

(3) The ECAP-processed Al–3%Mg–0.2%Sc, Al–3%Mg–0.2%Fe and Al–3%Mg–0.1%Zr alloys yielded maximum elongations of $\sim 640\%$, $\sim 370\%$ and $\sim 390\%$, respectively, when tested in tension at 523 K ($0.59T_m$) with an initial strain rate of $3.3 \times 10^{-4} \text{ s}^{-1}$. Such elongations resulted in more than three times or about twice the elongation achieved in a binary Al–3%Mg alloy.

(4) Tensile testing of the Al–3%Mg–0.2%Fe and Al–3%Mg–0.1%Zr alloys at 573 K ($0.65T_m$) led to an insufficient ductility for superplasticity and this was due to significant grain growth at this temperature.

(5) The ECAP-processed Al–3%Mg–0.2%Sc also exhibited a maximum elongation of $\sim 420\%$ when tested in tension at 473 K ($0.54T_m$) with an initial strain rate of $3.3 \times 10^{-4} \text{ s}^{-1}$. This elongation was more than twice that achieved in the binary Al–3%Mg alloy and the temperature of 473 K is the lowest homologous temperature reported to date for superplasticity in Al-based alloys.

(6) The large ductilities achieved in the Al–3%Mg–0.2%Fe and Al–3%Mg–0.1%Zr alloys confirm that Fe and Zr may be used as alternative elements for Sc although their use is effectively limited to lower temperatures.

Acknowledgements

We are grateful to Mr. Takayoshi Fujinami for his helpful assistance. This study was supported in part by the Light Metals Educational Foundation of Japan and in part by the US

Army Research Office under Grant No. DAAD19-00-1-0488.

REFERENCES

- 1) T. G. Langdon: Metall. Trans. **13A** (1982) 689–701.
- 2) Y. Ma, M. Furukawa, Z. Horita, M. Nemoto, R. Z. Valiev and T. G. Langdon: Mater. Trans., JIM **37** (1996) 336–339.
- 3) R. Z. Valiev, N. A. Krasilnikov and N. K. Tsenev: Mater. Sci. Eng. **A137** (1991) 35–40.
- 4) T. C. Low and R. Z. Valiev (eds): Investigations and applications of severe plastic deformation, (Dordrecht, Kluwer, 2000).
- 5) R. Z. Valiev, R. K. Islamgaliev and I. V. Alexandrov: Prog. Mater. Sci. **45** (2000) 103–189.
- 6) V. M. Segal, V. I. Reznikov, A. E. Drobysheskiy and V. I. Kopylov: Russ. Metall. **1** (1981) 99–105.
- 7) Y. Iwahashi, Z. Horita, M. Nemoto and T. G. Langdon: Acta Mater. **46** (1998) 3317–3331.
- 8) Y. Iwahashi, Z. Horita, M. Nemoto and T. G. Langdon: Metall. Mater. Trans. A **29A** (1998) 2503–2510.
- 9) Z. Horita, T. Fujinami and T. G. Langdon: Mater. Sci. Eng. **A318** (2001) 34–41.
- 10) R. Z. Valiev, O. A. Kaibyshev, R. I. Kuznetsov, R. Sh. Musalimov and N. K. Tsenev: Sov. Phys. Dokl. **33** (1988) 626–627.
- 11) The melting points of the Al–4 mass%Cu–0.5 mass%Zr and AZ91 Mg-based alloys were estimated from the Al–Cu and Mg–Al binary phase diagrams (*Alloy phase diagrams* edited by T. B. Massalski, American Society for Metals, (1987)) rather than using the melting points of pure Al and pure Mg: 863 K for the former alloy and 773 K for the latter alloy. These values are used to make the evaluation of the homologous testing temperatures more rigorous. No such estimation was attempted for the melting point of the Cu–38%Zn–3%Sn alloy as it was measured to be 1121 K in an earlier study by Neishi *et al.*¹³⁾
- 12) M. Mabuchi, H. Iwasaki, K. Yanase and K. Higashi: Scr. Mater. **36** (1997) 681–686.
- 13) K. Neishi, T. Uchida, A. Yamauchi, K. Nakamura, Z. Horita and T. G. Langdon: Mater. Sci. Eng. **A307** (2001) 23–28.
- 14) R. Z. Valiev, D. A. Salimonenko, N. K. Tsenev, P. B. Berbon and T. G. Langdon: Scr. Mater. **37** (1997) 1945–1950.
- 15) S. Lee, P. B. Berbon, M. Furukawa, Z. Horita, M. Nemoto, N. K. Tsenev, R. Z. Valiev and T. G. Langdon: Mater. Sci. Eng. **A272** (1999) 63–72.
- 16) P. B. Berbon, S. Komura, A. Utsunomiya, Z. Horita, M. Furukawa, M. Nemoto and T. G. Langdon: Mater. Trans., JIM **40** (1999) 772–778.
- 17) Z. Horita, M. Furukawa, M. Nemoto, A. J. Barnes and T. G. Langdon: Acta Mater. **48** (2000) 3633–3640.
- 18) S. Komura, Z. Horita, M. Furukawa, M. Nemoto and T. G. Langdon: Metall. Mater. Trans. A **32A** (2001) 707–716.
- 19) Y. Iwahashi, J. Wang, Z. Horita, M. Nemoto and T. G. Langdon: Scr. Mater. **35** (1996) 143–146.
- 20) M. Furukawa, Y. Iwahashi, Z. Horita, M. Nemoto and T. G. Langdon: Mater. Sci. Eng. **A257** (1998) 328–332.
- 21) H. Hasegawa, S. Komura, A. Utsunomiya, Z. Horita, M. Furukawa, M. Nemoto and T. G. Langdon: Mater. Sci. Eng. **A265** (1998) 188–196.
- 22) M. Furukawa, H. Wang and M. Nemoto: J. Jpn. Inst. Light Metals **40** (1990) 20–26.
- 23) S.-I. Fujikawa: J. Jpn. Inst. Light Metals **46** (1996) 202–215.
- 24) S. Lee, A. Utsunomiya, H. Akamatsu, K. Neishi, M. Furukawa, Z. Horita and T. G. Langdon: Acta Mater. **50** (2002) 553–564.